



Fabrication of flame-retardant, strong, and tough epoxy resins by solvent-free polymerization with bioderived, reactive flame retardant

Guofeng Ye^a, Siqi Huo^{b,c,*}, Cheng Wang^a, Qi Zhang^a, Bingtao Wang^d, Zhenghong Guo^d, Hao Wang^b, Zhitian Liu^{a,*}

^a Hubei Engineering Technology Research Center of Optoelectronic and New Energy Materials, School of Materials Science & Engineering, Wuhan Institute of Technology, Wuhan 430205, China

^b Centre for Future Materials, University of Southern Queensland, Springfield 4300, Australia

^c School of Engineering, University of Southern Queensland, Springfield 4300, Australia

^d Institute of Fire Safety Materials, NingboTech University, Ningbo 315100, China

ARTICLE INFO

Keywords:

Solvent-free polymerization
Bio-based flame retardant
Epoxy resin
 π - π stacking
Comprehensive properties

ABSTRACT

Replacing petroleum-derived chemicals with biobased ones to develop high-performance polymers is an important direction of sustainable development strategy. However, the current bio-based polymers suffered from complex preparation and unsatisfactory comprehensive properties. Herein, the bio-based 9,10-dihydro-10-(2,3-dicarboxypropyl)-9-oxa-10-phosphaphenanthrene 10-oxide (DDP) was covalently introduced into epoxy resin (EP)/anhydride system via solvent-free, green polymerization. The resulting EP_{1,2} sample (phosphorus content = 1.2 wt%) achieved a UL-94 V-0 rating with a limiting oxygen index (LOI) of 32.6%, indicative of outstanding flame retardancy. The peak heat release rate and total heat release of EP_{1,2} sample were 50.5% and 22.6% lower than virgin EP. DDP featured the *in-situ* reinforcing and toughening actions on EP due to the π - π stacking of its biphenyl group. The impact strength, tensile strength and elongation at break of EP_{1,2} were 218.2%, 46.5%, and 98.1% higher than those of EP, indicating exceptional mechanical strength and toughness. The high transparency and thermal stability of EP_{1,2} were well-preserved after adding DDP. Obviously, EP_{1,2} outperformed many previous flame-retardant EP systems due to its ease of fabrication and great overall performance. Therefore, this work offers a feasible and green strategy for the fabrication of advanced EPs with exceptional flame retardancy, mechanical properties, optical performances, and thermal stability by bioderived, reactive flame retardants, which is conducive to the sustainable development.

1. Introduction

Epoxy resin (EP), as an important polymeric material, is frequently used as an adhesive or matrix for composite materials employed in construction, transportation, and electrical equipment owing to its favourable adhesive properties, solvent resistance, and electrical insulation [1–3]. The amino- or anhydride-cured EPs are the most commonly applied epoxy systems in industry. The low viscosity, shrinkage and excellent electrical properties of the anhydride-cured EPs provide them broader applications in the electrical and aerospace fields [4,5]. However, the flame retardancy of the anhydride-cured EPs is poor, which limits their high-performance applications in these field [6–9]. The introduction of flame retardants (FRs) is a widespread method of solving the flammability problem for the anhydride-cured EPs, and the

phosphorus-containing flame retardant is one of the most promising FRs because it is environmentally-friendly and features high efficiency. For instance, Xu et al. designed a phosphorus-containing co-curing agent (DOPOMAH), and the DOPOMAH-containing EP obtained a UL-94 V-0 rating and a LOI of 32.8% at a high phosphorus content of 2.0 wt% [10]. The flame-retardant action of DOPOMAH was demonstrated by the formation of P-containing radicals (e.g., PO·, HPO· and HPO₂·) with a quenching function in the gas phase and the generation of phosphate-based compounds with a catalytic carbonization effect in the condensed phase. Chen et al. reported a co-curing agent (TMDB) with phosphorus, nitrogen and boron and applied it in the EP/methyl tetrahydrophthalic anhydride (MeTHPA). Their results showed that the resultant EP achieved a LOI value of 29.6% with a UL-94 V-0 rating when the TMDB content reached 15.1 wt% (phosphorus content: 1.0 wt

* Corresponding authors.

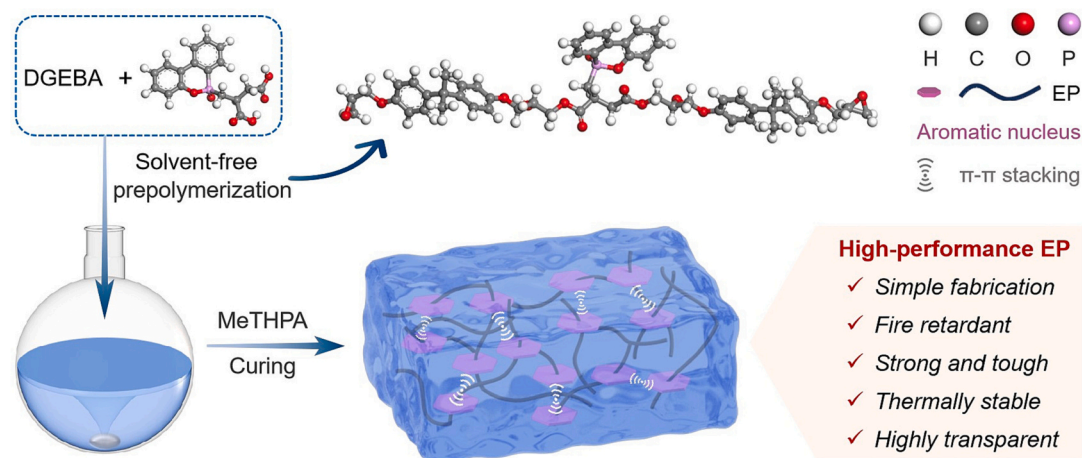
E-mail addresses: Siqi.Huo@unisq.edu.au (S. Huo), able.ztliu@wit.edu.cn (Z. Liu).

<https://doi.org/10.1016/j.susmat.2024.e00853>

Received 4 November 2023; Received in revised form 31 December 2023; Accepted 1 February 2024

Available online 2 February 2024

2214-9937/© 2024 The Authors. Published by Elsevier B.V. This is an open access article under the CC BY license (<http://creativecommons.org/licenses/by/4.0/>).



Scheme 1. Schematic diagram of solvent-free method for preparing high-performance EPs.

%) [4]. The co-action of phosphorus, nitrogen and boron in the char formation and radical quenching was the major factor in the improved flame retardancy. Apparently, these FRs can significantly improve the fire safety of EP thermosets, but their synthesis was complicated and involved the usage of abundant organic solvents and petroleum chemicals. In addition, the common phosphorus-containing FRs usually impart flame retardancy to EPs at the expense of mechanical properties and thermal stability due to their plasticizing and catalytic decomposition effects. To meet the sustainable development requirement, it is critical yet challenging in the manufacturing of high-performance, fire-retardant EPs combining superior thermal stability and mechanical properties by a facile and green method with bio-based additives [11].

Natural organisms have self-optimized over millions of years during evolution. Their distinct biological structures provide inspiration for material design [12,13]. Research works on DNA have shown that the non-covalent bonds can act as sacrificial bonds, which dissipate lots of energy before fracture, thus improving the toughness significantly [14,15]. Meanwhile, the non-covalent bonds can form physical cross-linking, therefore increasing the mechanical strength to some extents [16]. Hence, the formation of non-covalent interaction as sacrificial bond is a promising method to improve the mechanical strength and toughness of polymeric materials. However, there are few reports that develop mechanically-robust and tough EP systems by introducing the non-covalent interaction.

DDP is a bio-based, commercial chemical, which is produced *via* the Michael addition reaction of bioderived itaconic acid with 9,10-dihydro-9-oxa-10-phosphaphenanthrene 10-oxide (DOPO) [17]. DDP contains both carboxyl and phosphaphenanthrene groups, therefore we suppose that it can be as a flame-retardant co-curing agent for the EP/anhydride systems. Notably, there is a biphenyl group in the structure of DDP, and thus the DDP molecules are expected to form the π - π interactions. Based on the strategy of *in-situ* strengthening and toughening by sacrificial bond, covalently linking the bio-based DDP to the polymer network of the EP/anhydride system shows great promise for solving the trade-off between flame retardancy and mechanical properties. What's more, such preparation is simple and only involves the solvent-free polymerization.

Aiming to obtain the high-performance EPs by simple method, we used the solvent-free polymerization to covalently introduce the bio-based DDP into epoxy cross-linked network in this work. Then, the impacts of DDP on the optical properties, flame retardancy, thermal stability and mechanical properties for EP/anhydride system were studied in detail. The flame-retardant, reinforcing, and toughening mechanisms of DDP were also studied through various tests. As expected, our results showed that the as-fabricated epoxy system featured excellent overall performances because of introducing phosphorus-

containing group and π - π stacking. Thus, this work opens a new era for the development of advanced EPs by facile and green strategy with bio-based ingredients.

2. Material and methods

2.1. Materials

DDP was provided by Jianchu Biomedical Co., Ltd. (Hubei, China). MeTHPA, 2,4,6-tris(dimethylaminomethyl)phenol (DMP-30), methylsuccinic acid (MSA) and DOPO were obtained from Energy Chemical Co., Ltd. (Shanghai, China). Diglycidyl ether of bisphenol-A (DGEBA, CYD-128) was supplied by Yueyang Baling Petrochemical Co., Ltd. (Hunan, China).

2.2. Preparation of EP samples

EP samples were fabricated *via* a facile, solvent-free polymerization, with the preparation process and formulas illustrated in Scheme 1 and Table S1, respectively. Under continuous stirring, DDP and DGEBA were reacted at 100 °C for 2 h, and then 0.2 g of the mixture was used for titration experiment. The titration results (see Table S2) confirmed that the carboxylic acid group of DDP was completely reacted with the epoxy group of DGEBA within 2 h. Subsequently, the curing agent (MeTHPA) and curing accelerator (DMP-30) were added into the resulting solution and mixed for 5 min at 75 °C. The molar ratio of carboxylic acid + anhydride to the epoxy group was 1:1. After defoaming for 3 min, the mixture was poured into in stainless-steel moulds and the mixture was cured at 80 °C and 130 °C for 5 h, respectively. The EP_x sample was obtained, and the x was representative of its phosphorus content. The EP/MSA and EP/DOPO, as control specimens, were fabricated in the same manner to explore the reasons for the enhanced mechanical properties of EP_{1,2}. Under the same sample mass, the molar amount of MSA in EP/MSA sample was the same as that of DDP in EP_{1,2} sample. The phosphorus content of EP/DOPO sample was 1.2 wt%, which was the same as that of EP_{1,2} sample. The molecular structures of DDP, MSA and DOPO are shown in Fig. S1.

2.3. Characterizations

Please see the Supporting Information.

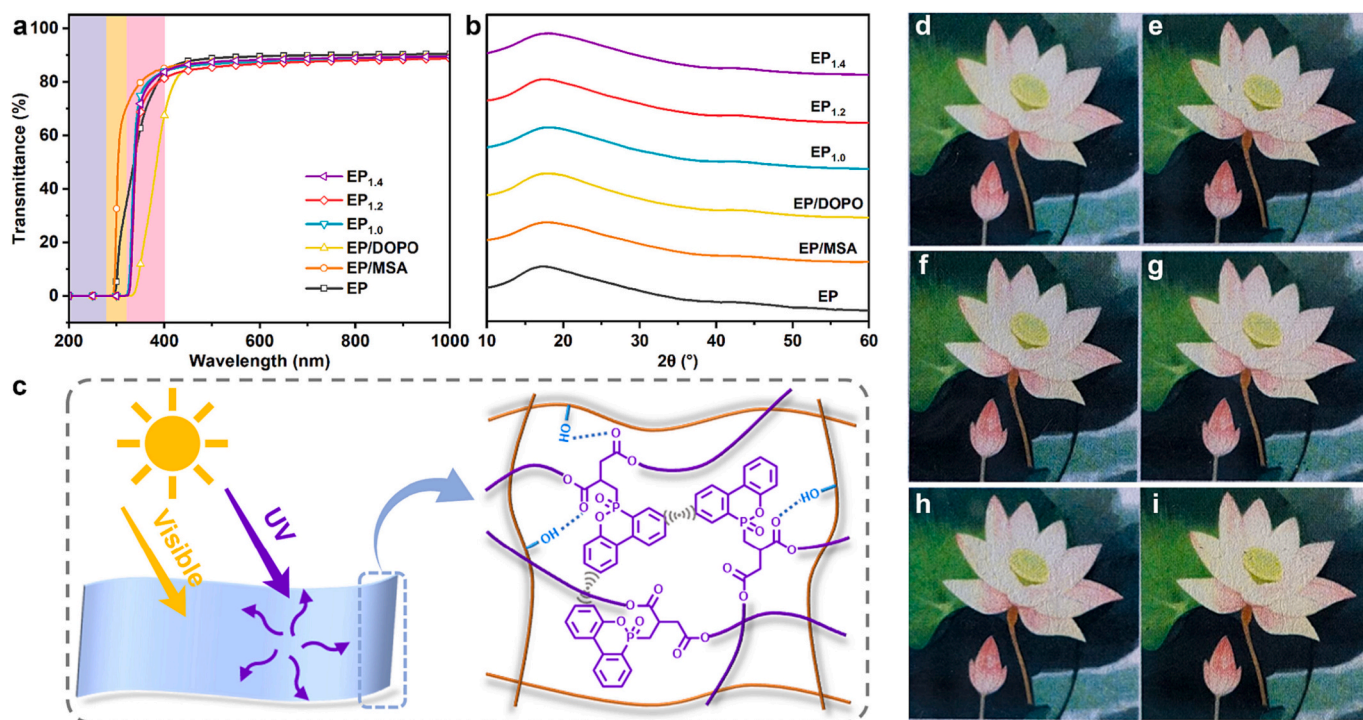


Fig. 1. (a) UV–visible transmission spectra and (b) X-ray diffraction patterns of EP samples; (c) illustration of possible mechanism for light transmission; and digital images of (d) EP, (e) EP_{1.0}, (f) EP_{1.2}, (g) EP_{1.4}, (h) EP/MSA and (i) EP/DOPO films.

3. Results and discussion

3.1. Optical properties

The impacts of DDP on the optical performance of EPs were characterized by UV–visible spectrophotometer and digital camera. EP_x exhibited considerable transparency (see Fig. 1d–g), which demonstrated that EP and DDP were well-compatible. As shown in Fig. 1a, the transmission for all EP specimens was enhanced with the wavelength, because the long wave transmitted through the sample more simply than short wave. The transmittance of EP_x samples was close to that of EP sample in the visible range of 500–1000 nm. For instance, EP and EP_{1.2} samples showed 90.3% and 88.7% transmittance at 800 nm, respectively (see Table S3). Such results confirmed that DDP can effectively maintain the high transparency of EP. It is well known that the reliability of polymeric materials in practical application is closely related to their UV resistance [18], therefore the transmittance in the UV region was studied in detail. In the range of 200 to 275 nm (UVC), the transmittance of all EP samples was 0. In the range of 275 to 320 nm (UVB), EP/MSA and EP exhibited high transmittance, but the transmittance of EP_x and EP/DOPO was still close to 0%. Similarly, EP_x and EP/DOPO exhibited better UV resistance than EP and EP/MSA at wavelengths from 320 to 340 nm. In summary, DDP maintained the excellent transparency for the resulting EP and enhanced the UV resistance.

The amorphous structure of EP is the main reason for its remarkable transparency [19]. Therefore, the effect of DDP upon the amorphous structure for EP was investigated via X-ray diffraction (XRD), with the patterns shown in Fig. 1b. No crystalline peak appeared in any XRD patterns except for the broadband diffraction peak at $2\theta = 17^\circ$. Apparently, DDP was uniformly dispersed within EP matrix by covalent bonding, and thus it did not affect the amorphous structure of EP, leading to a high transparency. In addition, due to the π - π stacking of biphenyl groups in DDP molecules, the EP_{1.0}, EP_{1.2} and EP_{1.4} samples featured improved UV resistance (see Fig. 1c) [20].

3.2. Flame retardancy

LOI, UL-94 and cone calorimeter test (CCT) were applied to evaluate the flame retardancy of EP samples. The LOI values and UL-94 ratings for EP specimens are listed in Fig. 2a. EP failed the UL-94 test, and its LOI was only 19.5%, indicating that it was extremely flammable. Adding DDP had dramatically increased the LOI and UL-94 ratings for EP_x samples. Specifically, the EP_{1.2} sample with 1.2 wt% of phosphorus passed a UL-94 V-0 rating with a LOI of 32.6%, indicating that it was a self-extinguishing material. As the DDP content was further increased, the LOI of EP_{1.4} sample reached 34.2%. Like the neat EP, EP/MSA displayed a lower LOI of 19.2% and failed UL-94 rating. Such findings indicate that the superior flame retardancy of EP_x is mainly due to the introduction of phosphorus-containing group [21].

To investigate the flame-retardant durability of EP samples, the LOI reductions and mass losses of EP samples after UV and hydrothermal aging tests were calculated (see Characterizations in Supporting Information), with the data displayed in Fig. 2b, c. As shown in Fig. S2, after different aging tests, the morphology and transparency of the EP/DOPO sample deteriorated, while those of EP_x samples were well maintained. Notably, besides achieving the UL-94 V-0 classification, the EP_{1.2} sample exhibited lower LOI reductions than EP and EP/DOPO samples after testing (see Fig. 2b and Table S4), indicative of better flame-retardant durability. Moreover, EP_{1.2} showed decreased mass losses relative to EP/DOPO, suggesting that the covalent bonding enhanced the reliability of EP_{1.2}. Obviously, the exceptional flame-retardant durability of EP_x is probably due to the crosslinking between DDP and EP matrix and the π - π stacking of biphenyl groups in DDP [3,22]. Therefore, the EP_x system with outstanding flame-retardant durability is expected to be widely applied in different industries.

In order to quantify the flame retardancy of EP samples [23–26], CCT was performed and the resulting curves and data are summarised in Fig. 2d–i and Table S5. As a result of the catalytic action of phosphorus-derived group in DDP [27], the time to ignition (TTI) values of EP_x were lower than that of EP (see Table S5). As illustrated in Fig. 2d, e, the incorporation of DDP greatly decreased the heat release of EP. To be

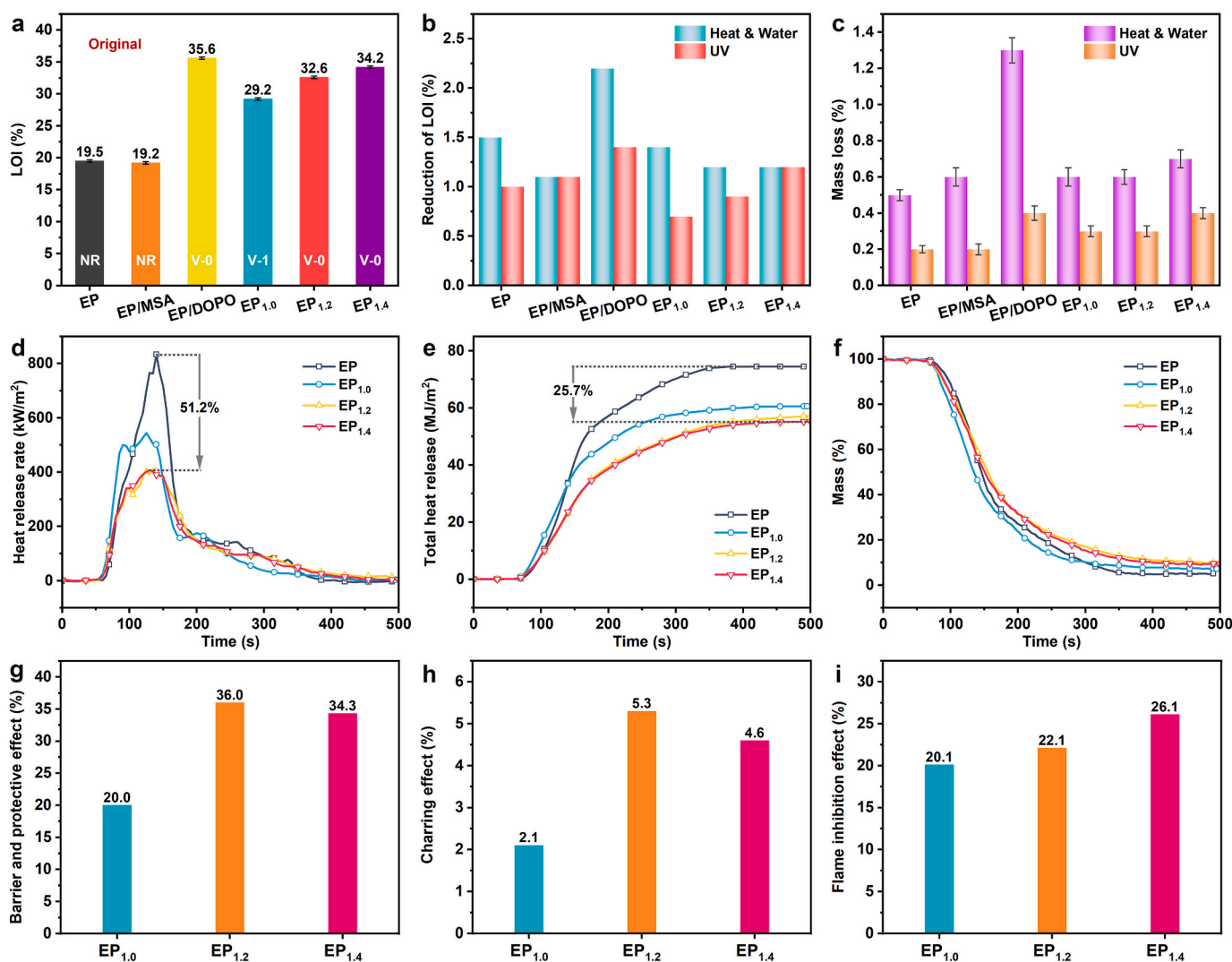


Fig. 2. (a) LOI and UL-94 results of EP samples; (b) LOI reduction, and (c) mass loss of EP samples after different durability tests; (d) heat release rate curves, (e) total heat release plots, and (f) mass loss curves of EP samples; and (g) barrier and protective effect, (h) charring effect, and (i) flame inhibition effect of EP_x samples.

specific, the peak heat release rate (PHRR) and total heat release (THR) of virgin EP were 833.3 kW/m² and 74.3 MJ/m² (see Table S5). In comparison, the PHRR and THR of EP_{1,4} sample were decreased to 406.8 kW/m² and 55.2 MJ/m², with reductions of 51.2% and 25.7%, respectively, compared with EP. As indicated in Fig. 2f and Table S5, the EP_x samples showed significantly higher char residues than virgin EP. In particular, the char residue of EP_{1,2} was increased from 4.9% of the neat EP to 9.9%, with a 102.0% enhancement. Apparently, DDP promoted charring of the EP matrix during burning. As can be seen in Fig. S3, the densification and expanded thickness of EP_{1,4} char were dramatically improved in comparison to EP char, providing further evidence of the condensed phase flame-retardant action of DDP [28,29]. The average effective heat of combustion (AEHC) is an important parameter to assess the degree of combustion of the gas-phase volatiles [30], with the values given in Table S5. The AEHC of EP_{1,4} was dropped from 19.9 MJ/kg of virgin EP to 14.7 MJ/kg. Thus, the pyrolytic components of DDP inhibited the combustion of volatiles in the gas phase, which resulted in an increase in incomplete burn [31]. The quenching action of phosphorus-containing groups in DDP is the main reason for the gas-phase fire suppression of the matrix.

According to previous works, the flame-retardant mechanism of FRs can be divided into three parts: barrier and protective effect (BPE), charring effect (CE) and flame inhibition effect (FIE) [32–34]. The first

two effects are on the condensed phase, and the last one is on the gaseous phase. The BPE, CE and FIE values of EP_x samples are listed in Fig. 2g–i. All EP_x samples displayed high BPE and FIE and low CE, which demonstrated that they mainly exerted barrier/protective and flame inhibition effects during combustion. Additionally, the FIE value was improved with the increasing phosphorus content, demonstrating the gradual enhancement of the gas-phase effect. In sum, DDP acted in both condensed and gas phases via barrier/protective and flame inhibition effects to suppress the heat release during combustion, thus enhancing the flame retardancy.

3.3. Flame-retardant mode-of-action

3.3.1. Condensed-phase mode-of-action

In order to investigate the flame-retardant mode-of-action of DDP in condensed phase, the proportion and structure of residual chars for EP and EP_{1,4} obtained from CCT were studied via Raman spectroscopy and X-ray photoelectron spectroscopy (XPS). As showed in Fig. 3a, the residual chars displayed the D and G bands at 1360 and 1605 cm⁻¹ corresponding to the unordered carbon and the orderly graphite structures respectively [35–37]. The graphitizing degree of residual char is directly proportionate to the integral area ratio of D to G bands (I_D/I_G). With the increasing DDP content, the I_D/I_G of residual char was reduced slowly,

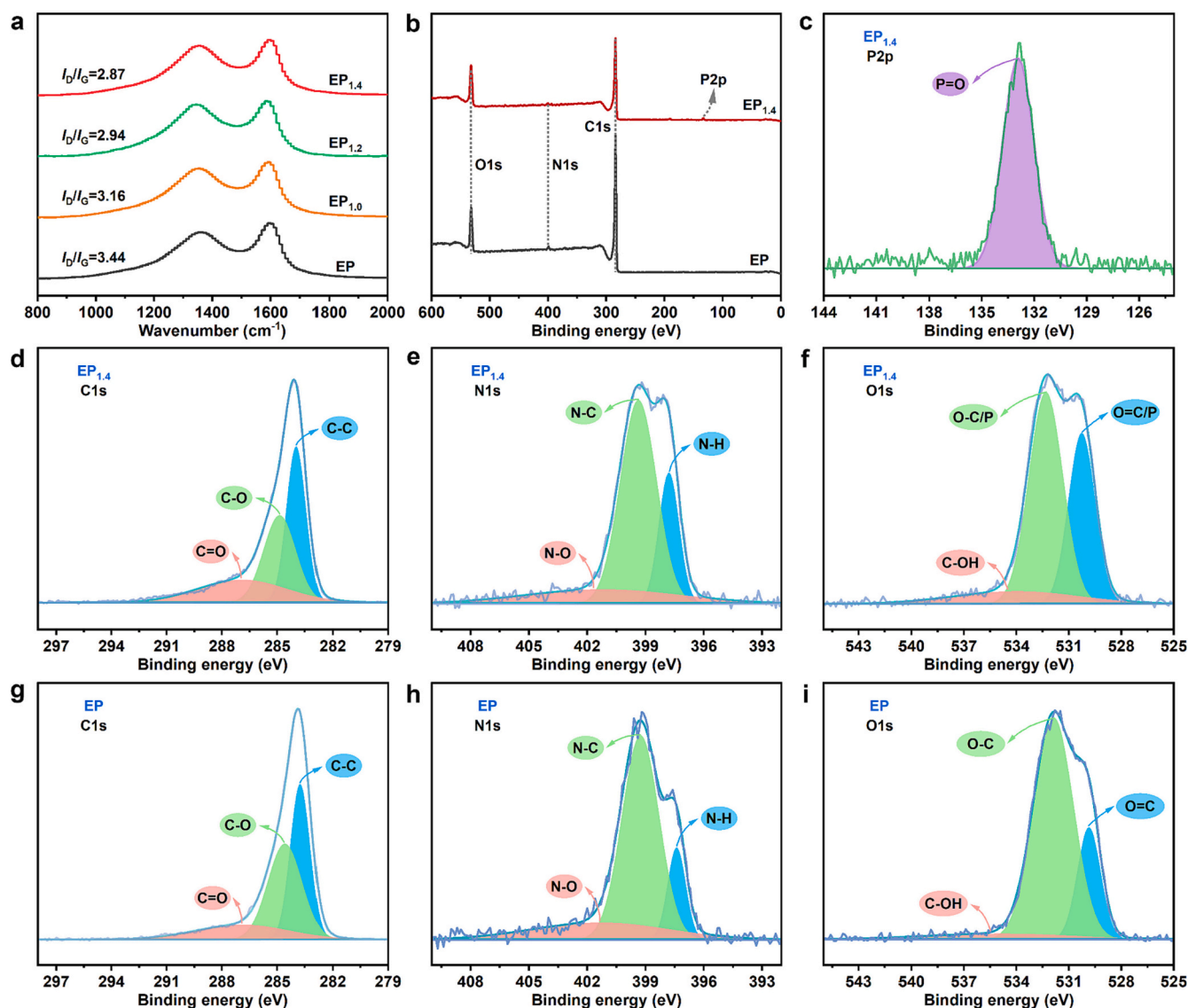


Fig. 3. (a) Raman spectra of residual chars for EP samples after cone calorimetry tests; (b) XPS survey spectra of residual chars for EP and EP_{1.4} after cone calorimetry tests; and high-resolution XPS (c) P2p, (d) C1s, (e) N1s, and (f) O1s spectra of residual char for EP_{1.4} and (g) C1s, (h) N1s, and (i) O1s spectra of residual char for EP after cone calorimetry tests.

which suggested that the degree of graphitisation of the char was increased. During combustion, DDP facilitated the charring of the EP matrix and increased the degree of graphitization of the residual char, which inhibited the release of heat.

The XPS data of EP and EP_{1.4} chars are presented in Fig. 3b-i, Table S6. Based on Fig. 3b and Table S6, the char of EP included the elements C (80.28 wt%), N (1.90 wt%) and O (17.82 wt%). Three deconvoluted peaks belonging to C—C, C—O and C=O were observed in the C1s spectrum of EP char (see Fig. 3g); the N1s spectrum of EP char showed three characteristic peaks, corresponding to -N-O-, -N-C- and -NH- (see Fig. 3h); and three deconvoluted peaks assigned to C-OH, O—C and O=C were also observed in the O1s spectrum of EP char (see Fig. 3i) [19]. In addition to the elements C, N and O, the element P (3.02 wt%) can be easily identified in the char of EP_{1.4} (see Fig. 3b and Table S6). In the C1s, N1s and O1s spectra, the EP_{1.4} char showed similar deconvoluted peaks to the EP char (see Fig. 3d-f). The P=O peak appeared in the P2p spectrum of EP_{1.4} char as presented in Fig. 3c, indicating that the pyrolysis products of DDP were in the form of phosphate derivatives in the condensed phase. Meanwhile, the O content of EP_{1.4} char was increased from 17.82 wt% of char for EP to 22.78 wt%, indicating that the P-

containing groups of DDP had interacted with the O-containing groups of the EP matrix during combustion, leaving higher O content in the char. To summarise, the phosphate-based decomposition products of DDP encouraged the EP matrix to generate a dense and expanding char layer with a high degree of graphitisation on its surface during combustion, inhibiting heat exchange and shielding the embedded matrix, thereby improving flame retardancy.

3.3.2. Gaseous-phase mode-of-action

Pyrolysis-gas chromatography/mass spectrometry (Py-GC/MS) test of DDP was performed to investigate the gaseous pyrolysis products of DDP under heating. The total ion chromatogram of DDP is shown in Fig. S4, and the major pyrolysis products are summarised in Table S7. DOPO, aromatic, biphenyl and carboxylic acid derivatives were the main pyrolysis products of DDP. The MSA-derived group in DDP was pyrolyzed to generate carboxylic acid and anhydride derivatives at retention time of 6.90, 12.13 and 16.59 min (see Table S7). Once the retention time exceeded 12.5 min, numerous biphenyl-containing fractures ($m/z = 154, 158, 170$ and 178) were observed, indicating the pyrolysis of DOPO-derived groups. Apparently, the formation of

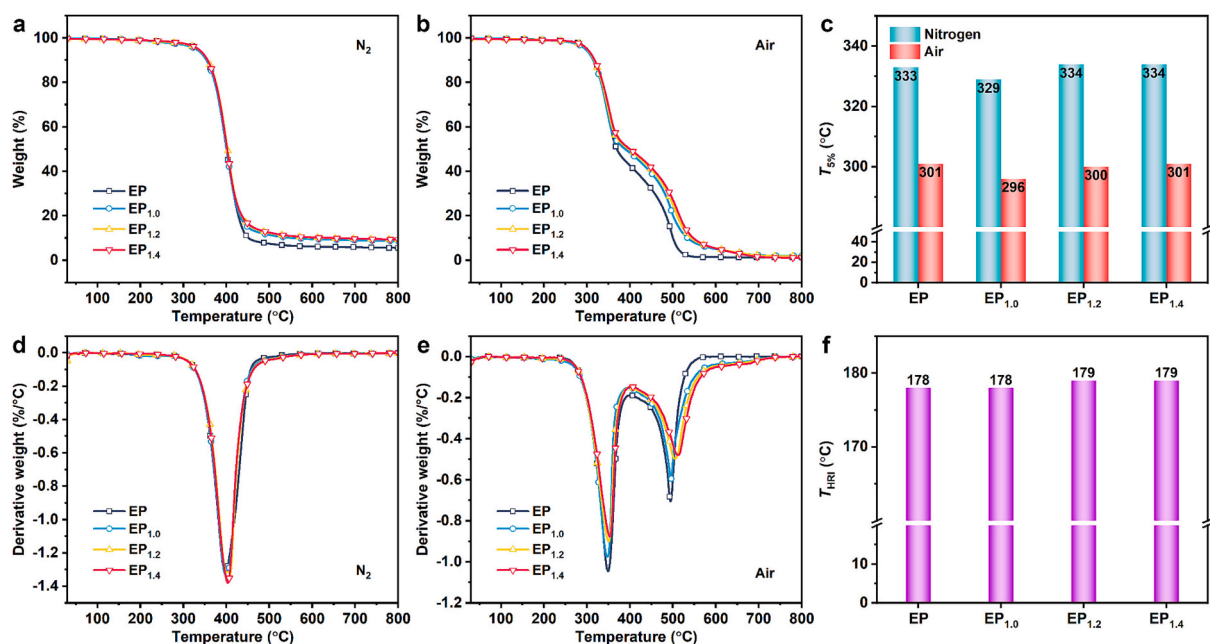


Fig. 4. Thermogravimetric (TG) curves of EP samples under (a) nitrogen and (b) air atmosphere; (c) temperature at 5% weight loss ($T_{5\%}$) values of EP samples under nitrogen and air atmosphere; derivative thermogravimetric (DTG) curves of EP samples under (d) nitrogen and (e) air atmosphere; and (f) heat-resistance index (T_{HRI}) values of EP samples.

biphenyl-containing fractures was associated with the generation of phosphorus-containing radicals ($PO\cdot$, $HPO\cdot$ and $HPO_2\cdot$) that were able to trap the high-energy radicals in the gaseous phase during combustion [38]. Based on the CCT and Py-GC/MS results, the gas-phase mode-of-action of DDP was primarily associated with the radical quenching for P-containing pyrolysis fragments [39,40].

3.4. Thermal stability

The thermogravimetric analysis (TGA) of EP samples was carried out in N₂ and air atmosphere respectively, with the plots and data provided in Fig. 4 and Table S8. In Fig. 4a-c and Table S8, the temperature at 5% weight loss ($T_{5\%}$) values of EP_x samples were basically the same to those of pure EP sample in both N₂ and air atmosphere. For example, the $T_{5\%}$ values of EP were 333 and 301 °C under N₂ and air, and those of EP_{1.4} were 334 and 301 °C. Additionally, the heat-resistance index (T_{HRI}) values of all EP samples were calculated based on previous works to further evaluate their thermal stability [41–43], with the results listed in Fig. 4f. Obviously, the T_{HRI} values of EP_x samples maintained at the same level as that of virgin EP. The above results demonstrated that the introduction of DDP did not affect the thermal stability of EP, making it superior to many common phosphorus-derived FRs because most of them deteriorated the thermal stability due to their catalytic decomposition effect. As presented in Fig. 4d, e and Table S8, the temperature at maximum weight loss rate (T_{max}) values of EP_x samples were higher than those of virgin EP, and showed an increasing trend with the increasing phosphorus content under both N₂ and air atmosphere, further confirming the well-maintained thermal stability. Notably, under N₂ flow, the char yield (CY) values of EP_x samples were significantly higher than those of EP sample. For example, the CY of EP_{1.2} sample was as high as 9.3%, with an increase of 69.1% relative to that of EP. Such result confirmed that DDP facilitated the carbonization of the EP matrix at high temperatures. In summary, the introduction of DDP effectively maintained the thermal stability of EP and significantly enhanced the char-forming ability.

3.5. Mechanical properties

The storage modulus (E') and tan delta are presented in Fig. S5 obtained from the dynamic mechanical analysis (DMA) test. The crosslink density (ν) of epoxy thermoset is calculated from the classical theory of rubber [44–46] (see Characterizations in Supporting Information). The E' at 30 °C, ν and T_g values of EP samples are provided in Table S9. In Fig. S5a and Table S9, the E' at 30 °C of EP_x was increased as DDP was added, confirming that introducing rigid phosphaphenanthrene group enhanced the rigidity [47]. The T_g values of EP_x samples were reduced due to the introduction of DDP, which was related to the decrease in ν (see Table S9). In general, DDP with a rigid phosphorus-containing group improved the mechanical rigidity of EP.

The impacts of DDP, MSA and DOPO on the mechanical performance of EP were investigated, with the results summarised in Fig. 5a-c and Table S9. The impact strength (α_k), tensile strength (σ), elongation at break (δ) and toughness of EP sample were 2.2 kJ/m², 58.1 MPa, 5.3% and 1.6 MJ/m³, respectively. The mechanical performance of EP_x was better than those of EP, EP/MSA and EP/DOPO samples (see Fig. 5a, b). For example, the α_k , σ , δ and toughness of EP_{1.2} sample reached 7.0 kJ/m², 85.1 MPa, 10.5% and 5.7 MJ/m³, which were 218.2%, 46.5%, 98.1% and 256.3% higher than those of virgin EP (see Table S9). In addition, the critical stress intensity factor (K_{IC}) and critical energy release rate (G_{IC}) exhibited similar variation trends, with EP_{1.2} and EP/DOPO showing the highest and lowest fracture toughness, respectively (see Fig. 5c). Consequently, DDP endowed EP with significantly-enhanced rigidity, robustness, and toughness. However, the EP_{1.4} sample exhibited reduced mechanical properties compared with EP_{1.2} and EP_{1.0} samples because of the introduction of excessive reactive flame retardant (DDP). Moreover, the impact strengths of EP samples after hydrothermal and UV aging tests were also investigated (see Table S4). DDP formed covalent bonds with the EP matrix during curing, and thus the EP_x samples showed low reductions in impact strengths after hydrothermal and UV aging. For example, the impact strengths of EP_{1.2} after hydrothermal and UV aging were 6.4 and 6.6 kJ/m², which were close to the original impact strength (7.0 kJ/m²). Therefore, the EP_{1.2} sample demonstrated significantly improved mechanical properties with the incorporation of the bio-based, reactive DDP.

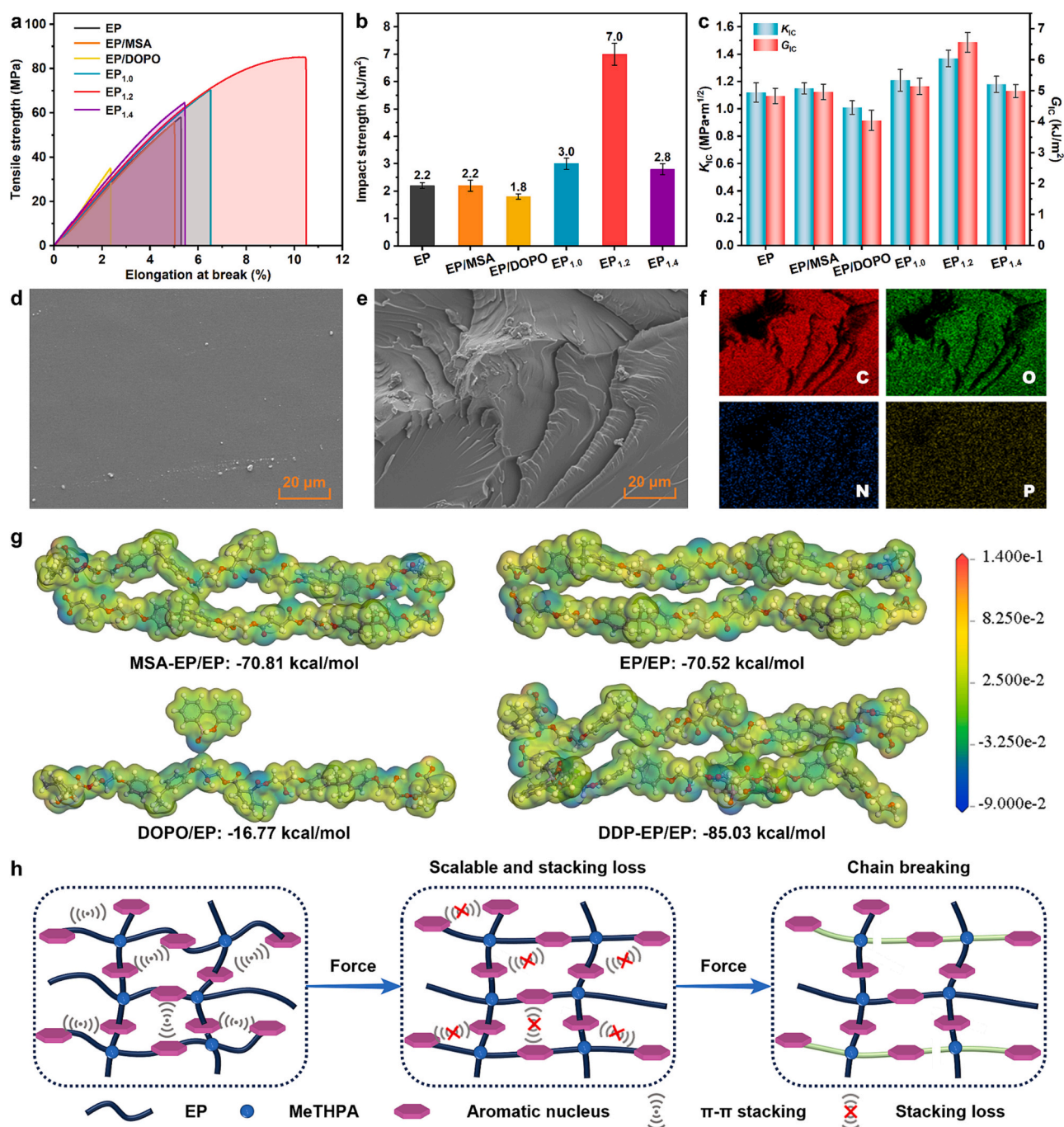


Fig. 5. (a) Tensile stress-strain curves, (b) impact strengths, and (c) critical stress intensity factor (K_{IC}) and critical energy release rate (G_{IC}) values of EP samples; SEM images of fractured surfaces for (d) EP, and (e) EP_{1.2}, and (f) the elemental mappings of EP_{1.2} sample after the Izod impact tests; (g) calculated electrostatic potentials and interaction energy for MSA-EP/EP, EP/EP, DOPO/EP and DDP-EP/EP; and (h) potential reinforcing and toughening mechanisms.

The fracture surface morphology of EP samples was investigated by scanning electron microscope (SEM) to validate the reinforcing and toughening mechanisms. The SEM images of cross-sections for EP samples from the Izod impact tests are presented in Fig. 5d, e and S6. The EP, EP/MSA, and EP/DOPO samples exhibited smooth fracture surfaces (see Fig. 5d and S6e, f), reflecting typical brittleness behaviour. In comparison, the fracture surfaces of EP_{1.0}, EP_{1.2} and EP_{1.4} became rough (see Fig. S6b-c and 5e) due to the introduction of DDP. Furthermore, the distinctive shearing bands can be observed on the fracture surface of EP_{1.2}. In addition, there were homogeneous distributions of C, O, N and P atoms in the EP_{1.2} fracture surface, suggesting that the homogeneous dispersion of DDP was a critical factor for the enhanced mechanical

properties of EP_{1.2}. The presence of shearing band indicated the *in-situ* strengthening and toughening actions of DDP [38,48]. To further investigate the microstructures of EP samples, their fracture surfaces were etched by *N,N*-dimethylacetamide for 24 h and then also characterized by SEM. The etched fracture surfaces are shown in Fig. S7. EP, EP/MSA and EP/DOPO displayed single-phase structures with relatively smooth surfaces (see Fig. S7a, e, and f). No obvious cavity and phase separation structure were observed within the etched surfaces of EP_{1.0} and EP_{1.2} samples (see Fig. S7b, c). Moreover, the C, O, N and P atoms were also evenly dispersed within the EP_{1.2} surface after etching (see Fig. S8). All these results confirmed that the covalent bonding enabled DDP to uniformly disperse within the EP matrix, thus realizing

Table 1Comparison of preparation process, mechanical properties, and thermal stability for EP_{1,2} and previously-reported EP/anhydride samples with a UL-94 V-0 rating.

Reference	Bio-based source	Synthesis step	Organic solvent used	Variation in $T_{5\%}$ (°C)	Variation in α_k (%)	Variation in σ (%)	Variation in δ (%)
[4]	No	3	1,4-Dioxane	-6.9	/	+31.8	+42.1
[8]	No	3	Ethanol, methanol, toluene, dichloromethane, n-hexane	-43.0	/	-0.5	/
[10]	No	1	Dimethylbenzene, tetrahydrofuran	-37.0	-4.8	-10.6	/
[51]	No	2	1,4-Dioxane	-83.0	+88.9	+39.5	/
[52]	No	1	/	-43.0	+5.0	/	/
[53]	No	2	1,4-Dioxane	-8.2	/	-1.9	-10.5
[54]	No	1	Acetone	-11.8	/	/	/
[55]	No	1	Propanoic acid, ethanol, acetic acid	-67.3	-27.1	-4.0	/
[56]	No	2	Tetrahydrofuran, 1,4-dioxane, n-hexane, ethyl ether	-47.0	+71.4	+27.6	-7.4
This work	Yes	0	No	+1.0	+218.2	+46.5	+98.1

dissipation of energy during the fracture process. In contrast, the etched section of EP_{1,4} showed obvious cavities (see Fig. S7d), which suggested that adding excessive DDP deteriorated the chemical bonding between it and the matrix, leading to the reduced mechanical properties [49]. Furthermore, the density functional theory (DFT) calculations of EP/EP, MSA-EP/EP, DOPO/EP and DDP-EP/EP were applied to further investigate the strengthening and toughening mechanisms of DDP (see Fig. 5g). DOPO/EP showed the highest binding energy of -16.77 kcal/mol; MSA-EP/EP and EP/EP exhibited similar binding energies of about -71 kcal/mol; and EP-DDP/EP displayed the lowest binding energy of -85.03 kcal/mol. Comparing the binding energies of EP samples, it was easy to find that the covalent bonding between DDP and EP matrix and the π - π conjugation between DDP molecules were the major reasons for the decrease in the binding energy and the enhancement in the mechanical properties [50]. The reactive DDP extended the polymer chains of EP_x samples, and enhanced the flexibility of the cross-linked network, leading to the improved toughness. What's more, the π - π conjugation between the DDP molecules absorbed part of the energy when the EP matrix was exposed to an extraneous force, resulting in energy dissipation (see Fig. 5h) and realizing *in-situ* reinforcing and toughening. Therefore, the covalent bonding between DDP and EP and the intermolecular π - π conjugation of DDP effectively improved the robustness, stiffness and toughness of EP.

3.6. Comprehensive comparison

The preparation process, thermal stability and mechanical properties of EP_{1,2} and previous EP/anhydride samples with a UL-94 V-0 classification were compared in Table 1 and Fig. S9. Obviously, DDP is a bio-based, environmentally-friendly flame retardant, and the fabrication of the DDP-containing EP_{1,2} only involves the well-designed, solvent-free polymerization, which is highly in line with the sustainable, green development strategy. What's more, the DDP-containing EP_{1,2} featured not only well-maintained thermal stability ($T_{5\%}$), but also significantly-enhanced mechanical performances (α_k , δ and σ), making it superior to many previous fire-safe EP/anhydride systems prepared by petroleum-based FRs (see Table 1 and Fig. S9b), thus able to find ubiquitous applications in modern industries [4,8,10,51–56]. The high transmittance and great flame-retardancy can also be observed from EP_{1,2} sample (see Fig. S9a). Overall, EP_{1,2} fabricated by the bio-based, reactive DDP is a high-performance epoxy system, which features facile preparation, and outstanding optical properties, thermal stability, mechanical performances and flame retardancy.

4. Conclusions

In this work, a high-performance EP system was prepared by facile, solvent-free polymerization with a bio-based, environmentally-friendly DDP. When the phosphorus content was ≤ 1.2 wt%, the flame

retardancy, mechanical performances and UV-blocking properties of the as-prepared EP_x samples were markedly improved, and the high thermal stability and transparency were effectively maintained. Even after different aging tests, the EP_{1,2} sample still exhibited superior flame-retardant and mechanical properties owing to the covalent bonding between DDP and epoxy cross-linking network. During combustion, DDP promoted the matrix carbonization in the condensed phase and acted as a trapping agent for the high-energy radicals in the gas phase, thus improving the flame retardancy. The obvious improvements in the mechanical properties of EP_{1,2} sample were mainly attributed to the chemical linkage between DDP and cross-linked network and the intermolecular π - π conjugation of DDP molecules. Thus, this work delivers an environmentally-friendly and integrated strategy for the fabrication of multifunctional EPs by bio-based, reactive FRs, which is anticipated to facilitate the development of sustainable bio-based FRs.

CRedit authorship contribution statement

Guofeng Ye: Data curation, Investigation, Writing – original draft. **Siqi Huo:** Conceptualization, Methodology, Writing – review & editing, Project administration. **Cheng Wang:** Investigation. **Qi Zhang:** Data curation. **Bingtao Wang:** Data curation. **Zhenghong Guo:** Data curation. **Hao Wang:** Supervision. **Zhitian Liu:** Project administration, Supervision.

Declaration of competing interest

The authors declare that they have no known competing financial interests or personal relationships that could have appeared to influence the work reported in this paper.

Data availability

Data will be made available on request.

Acknowledgements

This work was funded by the Australian Research Council Discovery Early Career Researcher Award (DE230100616), the Foundation for Outstanding Youth Innovative Research Groups of Higher Education Institution in Hubei Province (T201706), the Foundation for Innovative Research Groups of Hubei Natural Science Foundation of China (2017CFA009), and the Major Project of Ningbo Technology Innovation 2025 (2022Z113).

Appendix A. Supplementary data

Supplementary data to this article can be found online at <https://doi.org/10.1016/j.susmat.2024.e00853>.

References

- [1] J. Wang, S. Huo, J. Wang, S. Yang, K. Chen, C. Li, D. Fang, Z. Fang, P. Song, H. Wang, Green and facile synthesis of bio-based, flame-retardant, latent imidazole curing agent for single-component epoxy resin, *ACS Appl. Polym. Mater.* 4 (5) (2022) 3564–3574, <https://doi.org/10.1021/acsapm.2c00138>.
- [2] J.-H. Chen, B.-W. Liu, J.-H. Lu, P. Lu, Y.-L. Tang, L. Chen, Y.-Z. Wang, Catalyst-free dynamic transesterification towards a high-performance and fire-safe epoxy vitrimer and its carbon fiber composite, *Green Chem.* 24 (18) (2022) 6980–6988, <https://doi.org/10.1039/d2gc01405j>.
- [3] G. Ye, S. Huo, C. Wang, P. Song, Z. Fang, H. Wang, Z. Liu, Durable flame-retardant, strong and tough epoxy resins with well-preserved thermal and optical properties via introducing a bio-based, phosphorus-phosphorus, hyperbranched oligomer, *Polym. Degrad. Stab.* 207 (2023) 110235, <https://doi.org/10.1016/j.polymdegradstab.2022.110235>.
- [4] Y. Chen, H. Duan, S. Ji, H. Ma, Novel phosphorus/nitrogen/boron-containing carboxylic acid as co-curing agent for fire safety of epoxy resin with enhanced mechanical properties, *J. Hazard. Mater.* 402 (2021) 123769, <https://doi.org/10.1016/j.jhazmat.2020.123769>.
- [5] F. Li, S. Nan, R. Zhu, R. Yao, H. Wang, T. Zhang, J. Zhang, Abundant octadecylamine modified epoxy resin for superhydrophobic and durable composite coating, *Sustain. Mater. Technol.* 37 (2023) e00690, <https://doi.org/10.1016/j.susmat.2023.e00690>.
- [6] Q. Yang, J. Wang, X. Chen, S. Yang, S. Huo, Q. Chen, P. Guo, X. Wang, F. Liu, W. Chen, P. Song, H. Wang, A phosphorus-containing tertiary amine hardener enabled flame retardant, heat resistant and mechanically strong yet tough epoxy resins, *Chem. Eng. J.* 468 (2023) 143811, <https://doi.org/10.1016/j.cej.2023.143811>.
- [7] T. Ma, L. Li, T. Liu, C. Guo, Synthesis of a caged bicyclic phosphates derived anhydride and its performance as a flame-retardant curing agent for epoxy resins, *Polym. Adv. Technol.* 30 (5) (2019) 1314–1324, <https://doi.org/10.1002/pat.4565>.
- [8] J. Cao, H. Duan, J. Zou, J. Zhang, C. Wan, C. Zhang, H. Ma, Bio-based phosphorus-containing benzoxazine towards high fire safety, heat resistance and mechanical properties of anhydride-cured epoxy resin, *Polym. Degrad. Stab.* 198 (2022) 109878, <https://doi.org/10.1016/j.polymdegradstab.2022.109878>.
- [9] H. Ma, P. Song, Z. Fang, Flame retarded polymer nanocomposites: development, trend and future perspective, *Sci. China Chem.* 54 (2) (2011) 302–313, <https://doi.org/10.1007/s11426-010-4196-4>.
- [10] Q. Xu, S. Zhang, Z. Su, D. Li, S. Liang, B. Li, T. Lian, X. Qin, M. Jiang, P. Liu, A novel 9,10-dihydro-9-oxa-10-phosphaphenanthrene-10-oxide-based reactive flame retardant for epoxy resin: synthesis, properties, and comparison, *J. Appl. Polym. Sci.* 139 (8) (2021) e51688, <https://doi.org/10.1002/app.51688>.
- [11] Y. Liu, J. Liu, P. Song, Recent advances in polysaccharide-based carbon aerogels for environmental remediation and sustainable energy, *Sustain. Mater. Technol.* 27 (2021) e00240, <https://doi.org/10.1016/j.susmat.2020.e00240>.
- [12] C. Du, Y. Xu, C. Yan, W. Zhang, H. Hu, Y. Chen, M. Xu, C. Wang, B. Li, L. Liu, Facile construction strategy for intrinsically fire-safe and thermal-insulating bio-based chitosan aerogel, *Sustain. Mater. Technol.* 39 (2024) e00794, <https://doi.org/10.1016/j.susmat.2023.e00794>.
- [13] D. Glowacz-Czerwonka, P. Zakrzewska, M. Oleksy, K. Pielichowska, M. Kuznia, T. Tlejeko, The influence of biowaste-based fillers on the mechanical and fire properties of rigid polyurethane foams, *Sustain. Mater. Technol.* 36 (2023) e00610, <https://doi.org/10.1016/j.susmat.2023.e00610>.
- [14] S. Basu, R. Johl, S. Pacelli, S. Gehrke, A. Paul, Fabricating tough interpenetrating network Cryogels with DNA as the primary network for biomedical applications, *ACS Macro Lett.* 9 (9) (2020) 1230–1236, <https://doi.org/10.1021/acsmacrolett.0c00448>.
- [15] C.K. Lee, S.R. Shin, J.Y. Mun, S.-S. Han, I. So, J.-H. Jeon, T.M. Kang, S.I. Kim, P. G. Whitten, G.G. Wallace, G.M. Spinks, S.J. Kim, Tough Supersoft sponge fibers with tunable stiffness from a DNA self-assembly technique, *Angew. Chem. Int. Ed.* 48 (28) (2009) 5116–5120, <https://doi.org/10.1002/anie.200804788>.
- [16] Z. Tang, J. Huang, B. Guo, L. Zhang, F. Liu, Bioinspired engineering of sacrificial Metal-Ligand bonds into elastomers with supramolecular performance and adaptive recovery, *Macromolecules* 49 (5) (2016) 1781–1789, <https://doi.org/10.1021/acs.macromol.5b02756>.
- [17] E. Ozman, C. Dizman, H. Birtane, M.V. Kahraman, Novel bio-based phosphorus-containing UV-curable flame-retardant coatings, *J. Coat. Technol. Res.* 20 (4) (2023) 1257–1268, <https://doi.org/10.1007/s11998-022-00740-9>.
- [18] R. Heidrich, A. Mordvinkin, R. Gottschalg, Quantification of UV protecting additives in ethylene-vinyl acetate copolymer encapsulants for photovoltaic modules with pyrolysis-gas chromatography-mass spectrometry, *Polym. Test.* 118 (2023) 107913, <https://doi.org/10.1016/j.polymertesting.2022.107913>.
- [19] S. Huo, Z. Zhou, J. Jiang, T. Sai, S. Ran, Z. Fang, P. Song, H. Wang, Flame-retardant, transparent, mechanically-strong and tough epoxy resin enabled by high-efficiency multifunctional boron-based polyphosphonamide, *Chem. Eng. J.* 427 (2022) 131578, <https://doi.org/10.1016/j.cej.2021.131578>.
- [20] Y.-F. Ai, L. Xia, F.-Q. Pang, Y.-L. Xu, H.-B. Zhao, R.-K. Jian, Mechanically strong and flame-retardant epoxy resins with anti-corrosion performance, *Compos. Part B Eng.* 193 (2020) 108019, <https://doi.org/10.1016/j.compositesb.2020.108019>.
- [21] S. Jin, L. Qian, Y. Qiu, Y. Chen, F. Xin, High-efficiency flame retardant behavior of bi-DOPo compound with hydroxyl group on epoxy resin, *Polym. Degrad. Stab.* 166 (2019) 344–352, <https://doi.org/10.1016/j.polymdegradstab.2019.06.024>.
- [22] C. Wang, S. Huo, G. Ye, P. Song, H. Wang, Z. Liu, A P/Si-containing polythienimine curing agent towards transparent, durable fire-safe, mechanically-robust and tough epoxy resins, *Chem. Eng. J.* 451 (2023) 138768, <https://doi.org/10.1016/j.cej.2022.138768>.
- [23] Z. Ma, X. Liu, X. Xu, L. Liu, B. Yu, C. Maluk, G. Huang, H. Wang, P. Song, Bioinspired, highly adhesive, nanostructured polymeric coatings for Superhydrophobic fire-extinguishing thermal insulation foam, *ACS Nano* 15 (2021) 11667–11680, <https://doi.org/10.1021/acsnano.1c02254>.
- [24] F. Fang, S. Huo, H. Shen, S. Ran, H. Wang, P. Song, Z. Fang, A bio-based ionic complex with different oxidation states of phosphorus for reducing flammability and smoke release of epoxy resins, *Compos. Commun.* 17 (2020) 104–108, <https://doi.org/10.1016/j.coco.2019.11.011>.
- [25] Y. Sun, S. Sun, L. Chen, L. Liu, P. Song, W. Li, Y. Yu, L. Fengzhu, J. Qian, H. Wang, Flame retardant and mechanically tough poly(lactic acid) biocomposites via combining ammonia polyphosphate and polyethylene glycol, *Compos. Commun.* 6 (2017) 1–5, <https://doi.org/10.1016/j.coco.2017.07.005>.
- [26] P. Song, Y. Shen, B. Du, Z. Guo, Z. Fang, Fabrication of fullerene-decorated carbon nanotubes and their application in flame-retardant polypropylene, *Nanoscale* 1 (1) (2009) 118–121, <https://doi.org/10.1039/b9nr00026g>.
- [27] G. Ye, S. Huo, C. Wang, Q. Shi, L. Yu, Z. Liu, Z. Fang, H. Wang, A novel hyperbranched phosphorus-boron polymer for transparent, flame-retardant, smoke-suppressive, robust yet tough epoxy resins, *Compos. Part B Eng.* 227 (2021) 109395, <https://doi.org/10.1016/j.compositesb.2021.109395>.
- [28] T. Sai, S. Ran, Z. Guo, H. Yan, Y. Zhang, H. Wang, P. Song, Z. Fang, Transparent, highly thermostable and flame retardant polycarbonate enabled by rod-like phosphorus-containing metal complex aggregates, *Chem. Eng. J.* 409 (2021) 128223, <https://doi.org/10.1016/j.cej.2020.128223>.
- [29] Y. Xue, J. Feng, S. Huo, P. Song, B. Yu, L. Liu, H. Wang, Polyphosphoramide-intercalated MXene for simultaneously enhancing thermal stability, flame retardancy and mechanical properties of polylactide, *Chem. Eng. J.* 397 (2020) 125336, <https://doi.org/10.1016/j.cej.2020.125336>.
- [30] J. Feng, Y. Lu, H. Xie, Z. Xu, G. Huang, C.-F. Cao, Y. Zhang, V.S. Chevali, P. Song, H. Wang, Solvent-free synthesis of organic-inorganic Polyphosphoramide-Halloysite Nanohybrids for thermally stable and fire-resistant Polylactide, *ACS Sustain. Chem. Eng.* 10 (46) (2022) 15223–15232, <https://doi.org/10.1021/acssuschemeng.2c04899>.
- [31] M. Zhu, L. Liu, Z. Wang, Mesoporous silica via self-assembly of nano zinc aminotris-(methylene phosphonate) exhibiting reduced fire hazards and improved impact toughness in epoxy resin, *J. Hazard. Mater.* 392 (2020) 122343, <https://doi.org/10.1016/j.jhazmat.2020.122343>.
- [32] A. Zhang, J. Zhang, L. Liu, J. Dai, X. Lu, S. Huo, M. Hong, X. Liu, M. Lynch, X. Zeng, P. Burey, P. Song, Engineering phosphorus-containing lignin for epoxy biocomposites with enhanced thermal stability, fire retardancy and mechanical properties, *J. Mater. Sci. Technol.* 167 (2023) 82–93, <https://doi.org/10.1016/j.jmst.2023.06.004>.
- [33] S. Brehme, B. Schartel, J. Goebbels, O. Fischer, D. Pospiech, Y. Bykov, M. Döring, Phosphorus polyester versus aluminium phosphinate in poly(butylene terephthalate) (PBT): flame retardancy performance and mechanisms, *Polym. Degrad. Stab.* 96 (5) (2011) 875–884, <https://doi.org/10.1016/j.polymdegradstab.2011.01.035>.
- [34] J. Wang, L. Qian, Z. Huang, Y. Fang, Y. Qiu, Synergistic flame-retardant behavior and mechanisms of aluminum poly-hexamethylenephosphinate and phosphaphenanthrene in epoxy resin, *Polym. Degrad. Stab.* 130 (2016) 173–181, <https://doi.org/10.1016/j.polymdegradstab.2016.06.010>.
- [35] Q. Chen, L. Liu, A. Zhang, W. Wang, Z. Wang, J. Zhang, J. Feng, S. Huo, X. Zeng, P. Song, An iron phenylphosphinate/graphene oxide nanohybrid enabled flame-retardant, mechanically reinforced, and thermally conductive epoxy nanocomposites, *Chem. Eng. J.* 454 (2023) 140424, <https://doi.org/10.1016/j.cej.2022.140424>.
- [36] G. Yang, W.H. Wu, Y.H. Wang, Y.H. Jiao, L.Y. Lu, H.Q. Qu, X.Y. Qin, Synthesis of a novel phosphazene-based flame retardant with active amine groups and its application in reducing the fire hazard of epoxy resin, *J. Hazard. Mater.* 366 (2019) 78–87, <https://doi.org/10.1016/j.jhazmat.2018.11.093>.
- [37] J. Wang, X. Chen, J. Wang, S. Yang, K. Chen, L. Zhu, S. Huo, P. Song, H. Wang, High-performance, intrinsically fire-safe, single-component epoxy resins and carbon fiber reinforced epoxy composites based on two phosphorus-derived imidazoliums, *Polym. Degrad. Stab.* 208 (2023) 110261, <https://doi.org/10.1016/j.polymdegradstab.2023.110261>.
- [38] J. Zhang, X. Mi, S. Chen, Z. Xu, D. Zhang, M. Miao, J. Wang, A bio-based hyperbranched flame retardant for epoxy resins, *Chem. Eng. J.* 381 (2020) 122719, <https://doi.org/10.1016/j.cej.2019.122719>.
- [39] X. Hu, K.H. Wong, N.Y.G. Lai, H. Yu, J. Li, Effects of hexa (ethyl lactate)-cyclotriphosphazene on flame retardancy and mechanical properties of polylactide, *Sustain. Mater. Technol.* 38 (2023) e00708, <https://doi.org/10.1016/j.susmat.2023.e00708>.
- [40] Z. Yang, K. Wang, X. Wang, S. Huan, H. Yang, C. Wang, Low-cost, superhydrophobic, flame-retardant sunflower straw-based xerogel as thermal insulation materials for energy-efficient buildings, *Sustain. Mater. Technol.* 38 (2023) e00748, <https://doi.org/10.1016/j.susmat.2023.e00748>.
- [41] J. Gu, Z. Lv, Y. Wu, Y. Guo, L. Tian, H. Qiu, W. Li, Q. Zhang, Dielectric thermally conductive boron nitride/polyimide composites with outstanding thermal stabilities via in-situ polymerization-electrospinning-hot press method, *Compos. Part A: Appl. S.* 94 (2017) 209–216, <https://doi.org/10.1016/j.compositesa.2016.12.014>.
- [42] Z. Liu, J. Zhang, L. Tang, Y. Zhou, Y. Lin, R. Wang, J. Kong, Y. Tang, J. Gu, Improved wave-transparent performances and enhanced mechanical properties for fluoride-containing PBO precursor modified cyanate ester resins and their PBO

- fibers/cyanate ester composites, *Compos. Part B Eng.* 178 (2019) 107466, <https://doi.org/10.1016/j.compositesb.2019.107466>.
- [43] J. Gu, X. Yang, C. Li, K. Kou, Synthesis of cyanate Ester microcapsules via solvent evaporation technique and its application in epoxy resins as a healing agent, *Ind. Eng. Chem. Res.* 55 (41) (2016) 10941–10946, <https://doi.org/10.1021/acs.iecr.6b03093>.
- [44] N. Liu, H. Wang, B. Xu, L. Qu, D. Fang, Cross-linkable phosphorus/nitrogen-containing aromatic ethylenediamine endowing epoxy resin with excellent flame retardancy and mechanical properties, *Compos. Part A: Appl. S.* 162 (2022) 107145, <https://doi.org/10.1016/j.compositesa.2022.107145>.
- [45] Q. Zhang, J. Wang, S. Yang, J. Cheng, G. Ding, Y. Hu, S. Huo, Synthesis of a P/N/S-based flame retardant and its flame retardant effect on epoxy resin, *Fire Saf. J.* 113 (2020) 102994, <https://doi.org/10.1016/j.firesaf.2020.102994>.
- [46] Z. Hou, H. Cai, C. Li, B. Li, H. Wang, A phosphorus/silicon/triazine-containing flame retardant towards flame retardancy and mechanical properties of epoxy resin, *J. Appl. Polym. Sci.* 139 (31) (2022) e52712, <https://doi.org/10.1002/app.52712>.
- [47] N. Teng, J. Dai, S. Wang, X. Liu, J. Hu, X. Yi, X. Liu, Hyperbranched flame retardant to simultaneously improve the fire-safety, toughness and glass transition temperature of epoxy resin, *Eur. Polym. J.* 157 (2021) 110638, <https://doi.org/10.1016/j.eurpolymj.2021.110638>.
- [48] L. Zhong, Y. Hao, J. Zhang, F. Wei, T. Li, M. Miao, D. Zhang, Closed-loop recyclable fully bio-based epoxy Vitrimers from Ferulic acid-derived Hyperbranched epoxy resin, *Macromolecules* 55 (2) (2022) 595–607, <https://doi.org/10.1021/acs.macromol.1c02247>.
- [49] D. Chen, J. Li, Y. Yuan, C. Gao, Y. Cui, S. Li, H. Wang, C. Peng, X. Liu, Z. Wu, J. Ye, A new strategy to improve the toughness of epoxy thermosets by introducing the thermoplastic epoxy, *Polymer* 240 (2022) 124518, <https://doi.org/10.1016/j.polymer.2022.124518>.
- [50] Z. Deng, C. Tong, Z. Xin, X. Meng, M. Fan, W. Gong, C. Shu, Enhanced crystallization property and equilibrium mechanical properties of a novel self-assembly nucleating system based phosphate for polypropylene, *J. Polym. Res.* 29 (7) (2022) 297, <https://doi.org/10.1007/s10965-022-03157-5>.
- [51] H. Zhao, H. Duan, J. Zhang, L. Chen, C. Wan, C. Zhang, C. Liu, H. Ma, An Itaconic acid-based phosphorus-containing oligomer endowing epoxy resins with good flame Retardancy and toughness, *Macromol. Mater. Eng.* 308 (4) (2022), <https://doi.org/10.1002/mame.202200550>, 2200550.
- [52] Q. Li, Y. Li, Y. Chen, Q. Wu, S. Wang, An effective method for preparation of liquid phosphoric anhydride and its application in flame retardant epoxy resin, *Materials* 14 (9) (2021) 2205, <https://doi.org/10.3390/ma14092205>.
- [53] H. Duan, Y. Chen, S. Ji, R. Hu, H. Ma, A novel phosphorus/nitrogen-containing polycarboxylic acid endowing epoxy resin with excellent flame retardance and mechanical properties, *Chem. Eng. J.* 375 (2019) 121916, <https://doi.org/10.1016/j.cej.2019.121916>.
- [54] T. Ma, C. Guo, Synergistic effect between melamine cyanurate and a novel flame retardant curing agent containing a caged bicyclic phosphate on flame retardancy and thermal behavior of epoxy resins, *J. Anal. Appl. Pyrolysis* 124 (2017) 239–246, <https://doi.org/10.1016/j.jaap.2017.02.001>.
- [55] H. Zhang, M. Xu, B. Li, Synthesis of a novel phosphorus-containing curing agent and its effects on the flame retardancy, thermal degradation and moisture resistance of epoxy resins, *Polym. Adv. Technol.* 27 (7) (2016) 860–871, <https://doi.org/10.1002/pat.3722>.
- [56] G. Wang, Z. Nie, Synthesis of a novel phosphorus-containing epoxy curing agent and the thermal, mechanical and flame-retardant properties of the cured products, *Polym. Degrad. Stab.* 130 (2016) 143–154, <https://doi.org/10.1016/j.polymdegradstab.2016.06.002>.